The role of vapor fraction in hydrocarbon mist explosion

Stéphanie El-Zahlanieh, Amélie Jean, Alexis Vignes, Olivier Dufaud

HAL Id: ineris-03975699
https://ineris.hal.science/ineris-03975699

Submitted on 17 Apr 2023

The role of vapor fraction in hydrocarbon mist explosion

Stephanie El-Zahlanieh [a], Amélie Jean [a], Alexis Vignes [b] & Olivier Dufaud [a]

[a] Université de Lorraine, CNRS, LRGP, Nancy, France
[b] INERIS, Parc Technologique ALATA, BP 2, F-60550, Verneuil-en-Halatte, France

E-mail: *stephanie.el-zahlanieh@univ-lorraine.fr*

Abstract

The modern world depends greatly on hydrocarbons which are ubiquitous, indispensable fuels used in nearly every existing industry. Although important, their use may trigger dangerous incidents, whether in their production, handling, storage, or transporting phase, especially when aerosolized. In light of proposing a standard procedure to assess the flammability and explosivity of fuel mists, a new test method was established based on the EN 14034 standard. For the previous purposes, a gravity-fed mist generation system was designed and employed in a modified 20 L explosion vessel. This test method allowed the determination of the ignition sensitivity of several fuels. In addition, their explosion severity was represented by the explosion overpressure P_m, and the rate of pressure rise dP/dt_m, two thermo-kinetic parameters determined with a specifically developed control system and custom software. Nonetheless, a noticeable difference in the ignition sensitivity and the explosion severity was perceived when changing suppliers or petroleum cuts of some fuels. Moreover, sensitivity studies showed that both the droplet size distribution and the temperature of the droplets play a significant role in fuel mist explosion. These parameters can be directly related to the vapor fraction surrounding a droplet during its ignition. Consequently, this study focuses on the influence of varying the composition of three well-known and abundantly used fuels. Different petroleum cuts were introduced in different fractions into isooctane, Jet A1 aviation fuel, and diesel fuel mixtures which were then aerosolized into a uniformly distributed turbulent mist cloud and ignited using spark ignitors of 100 J. Subsequently, the same tests were executed in a vertical flame propagation tube coupled with a high-speed video camera allowing the visualization of the flame and the determination of the spatial flame velocity, and estimation of the laminar burning velocity. The latter was also estimated from the pressure-time evolution in the 20 L sphere using existing correlations. Indeed, the determination of the laminar burning velocity can be useful in modeling such accidents. Finally, highlighting the essential role of the mist and vapor fraction during their ignition has led to a better understanding of their explosion mechanisms.

Keywords: *mist, aerosol explosion, petroleum cuts, flame propagation, explosion severity, hybrid explosion*

1. Introduction

Over the years, the chemical and petrochemical sectors have seen a substantial number of explosions caused by liquid aerosol dispersions (Santon, 2009). These mist explosion incidents do not cease to take place and lead to human and material losses. Concerns over such incidents have grown as it became evident that they can occur at temperatures below the flashpoint of the aerosolized liquid (Eichhorn, 1955), and that, although the ATEX standards recognize the dangers of flammable mists, their categorization is still limited to this flashpoint. Indeed, while the classification of flammable gases and dust clouds is well-established, that of liquid aerosols remains less so. This is mainly due to a lack of scientific data and knowledge in such a matter.

The increased interest and concern in mitigating mist explosion incidents call for a standardized test method to evaluate such risks and for a greater understanding of the influence of external conditions. To address this issue, a test procedure based on the EN 14034 standard is proposed allowing the assessment of fuel mists' flammability and explosivity in a confined explosion vessel, well-known as the 20 L explosion sphere. Experiments were performed mainly on Jet A1 aviation fuel, B7 diesel fuel, and isooctane mists generated into the 20 L sphere using a Venturi-based spray nozzle. A considerable difference in ignitability was perceived, as fuel suppliers were changed or with the aging of the fuels. Therefore, in addition to the determination of the explosion severity, represented by the explosion overpressure (P_m) and the rate of pressure rise (dP/dt_m), and the ignition sensitivity, represented by the lower explosive limit (LEL) and the minimum ignition energy (MIE), this study emphasizes the influence of varying vapor fractions in the mist clouds on their ignitability and explosivity. Experiments were coupled with an evaporation model based on the d^2-law allowing the quantification of the liquid/vapor ratio in the 20 L sphere under specified conditions. Moreover, Jet A1 – methane hybrid mixtures were tested in order to specify different explosion regimes and highlight the contribution of the mist in such explosions. Complementary tests will be performed in a flame propagation tube allowing the estimation of the laminar burning velocity and its comparison to theoretical values calculated from the thermo-kinetic parameters.

2. Experiments

In the light of studying the influence of the vapor fraction on fuel mist ignitability and explosivity, experiments were carried out on binary isooctane-diesel blends, isooctane-Jet A1 blends, and hybrid mixtures of Jet A1 and methane gas. The blends were characterized by their flashpoint and compared by their ignition time $\tau_{ignition}$ and their explosion thermo-kinetic parameters P_m and dP/dt_m. MIE experiments were also performed to assess the ignitability of the mentioned blends. Hybrid explosion (Jet A1 + CH$_4$) experiments were, as well, carried out to identify explosion regimes and to pinpoint the contribution of mist in such explosions.

2.1   Tested fuels

The proposed test method, detailed in Section 2.2, was established using a variety of fuels (ethanol, isooctane, diesel, kerosene, biodiesel, light fuel oil, hydraulic oil). For this study, however, Jet A1 aviation fuel, B7 diesel fuel, and isooctane were the main focus as they are widely used in industries, and as they exhibit different physicochemical and thermodynamic properties. One should not overlook the involvement of these fuels in mist explosions. Indeed, diesel mist releases have caused a considerable number of explosions, notably in the marine sector (Reina del Pacifico, 1974, Miss Dorothy towing vessel, 2021, etc.) (Eckhoff, 2005; NTSB, 2022). Kerosene mist releases were involved in seven out of the 29 incidents reported by Santon (2009). Both fuels appeared in many incident reports, such as Lees et al. (2019) and Yuan et al. (2021). However, commercially available fuels, such as Jet A1 aviation fuel and B7 diesel fuel, have a wide range of compositions, making them difficult to investigate in-depth (Dumitrescu et al., 2011). Therefore, isooctane was introduced to both fuels to form a constant, easily quantifiable, vapor fraction allowing the comparison and understanding of their ignitability and explosivity.

Table 1 demonstrates the separate physicochemical properties of the three fuels following characterization tests such as the Hoeppler Falling-Ball viscometry, the Pendant Drop surface tension measurement, and the flashpoint determination using the Setaflash Series 3 flashpoint apparatus.

The following blends were prepared for this study:

- B7 diesel + 5, 7, 9, and 15 %$_{v/v}$ isooctane
- Jet A1 + 2, 5, 10, and 25 %$_{v/v}$ isooctane

Preliminary tests showed that the addition of isooctane had negligible effects on the physical properties of the mixture, and hence on the droplet size distribution. On the other hand, this addition triggered an important decrease in the flashpoint as shown in Figure 1 in the case of diesel-isooctane blends. Similar tendencies were observed for Jet A1-isooctane blends. It should be noted that the final

point at 100 %$_{v/v}$ isooctane is not experimental, as the flashpoint apparatus does not test for temperatures lower than 0 °C.

Table 1: *Physicochemical properties of Jet A1, diesel, and isooctane*

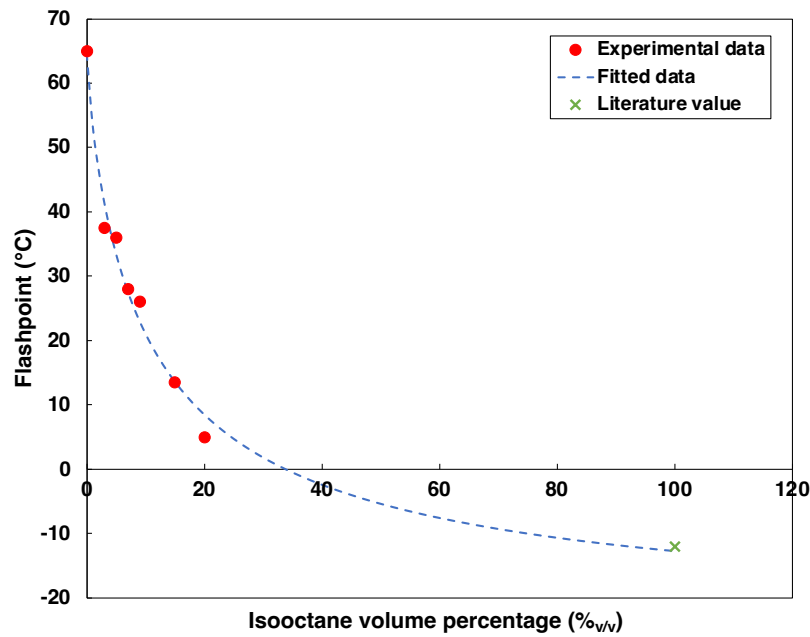| Fuel	Jet A1	Diesel B7	Isooctane
Density (kg.m^{-3})	840	880	690
Dyanmic viscosity (mPa.s)	1.2	2.95	0.45
Surface tension (kg.s^{-2})	0.026	0.027	0.018
Flashpoint (°C)	40	65	-12
Boiling point (°C)	130-300	150-390	99

Fig. 1. *Evolution of the flashpoint as a function of the volumetric percentage of isooctane in an isooctane-diesel blend*

For the evaporation model detailed in Sections 2.4 and 3.4, the vapor pressure of each of the three fuels was required to determine their vapor fractions. For these purposes, the following equations, found in literature, were used for each fuel:

- Jet A1:

$$P_{vap} = 5.76 \times 10^6 \cdot \exp\left(\frac{-4191}{T}\right) \qquad \text{(Shepherd et al., 1997)}$$

where P_{vap} is the vapor pressure in mbar, and T is the absolute temperature in K

- Diesel fuel:

$$\ln(P_{vap}) = 99.4943 - \frac{7332.14}{T} - 12.8127\ln(T) + 0.0128504T \qquad \text{(Safarov et al., 2018)}$$

where P_{vap} is in Pa, T is in K

- Isooctane:

$$\log P_{vap} = 3.93679 - \frac{1257.84}{T - 52.415} \qquad \text{(Willingham et al., 1945)}$$

where P_{vap} is in bar and T is in K

In the case of a mixture, Raoult's law $P = \sum_i P_i x_i$ is applied to measure the total vapor pressure with the assumption of an ideal solution based on the basic microscopic premise that intermolecular interactions between dissimilar molecules are equal to those between similar molecules and that their molar volumes are equal.

2.2 Ignitability and explosivity of fuel mist

As advised by the EN 14034 standard, the test apparatus employed in this study is the standardized 20 L explosion sphere. To mimic industrial leaks, a spray nozzle equipped with a Venturi junction was used to aerosolize the fuel into the sphere from the bottom. The injection duration and pressure were controlled using electronic valves, allowing the regulation of the mist's concentration, its droplet size distribution, and its level of turbulence, as well as the ignition delay. After injection, the mist cloud would then be instantaneously ignited (t_v = 3 ms) with a permanent spark of 100 J. Two piezoelectric pressure sensors allow the tracking of the pressure-time evolution during an explosion and then the determination of P_m and dP/dt_m using a specifically developed control and data acquisition system allowing the full control and safe operation of the explosion vessel and the optimal interpretation of the experimental data. An ignition is considered to take place when an overpressure of at least 0.5 bar relative to the initial pressure occurs, permitting the determination of both the lower explosive limit (LEL) and the minimum ignition energy (MIE).

All the experiments performed for this study were carried out using a spray nozzle of an orifice diameter of 0.45 mm and an injection pressure of 2.9 bar, ensuring a uniformly distributed mist cloud of median diameters varying between 8 and 10 μm and a constant turbulence level. Concentrations were limited to about 160 g.m^{-3} in order to avoid long injection durations, which enhance coalescence, sedimentation, or droplet-droplet interactions. Indeed, concentrations in this study are expressed as the injected mass divided by the vessel's volume. However, an exact estimation of the concentration in the sphere is required.

2.3 Flame propagation

Researchers like Burgoyne & Cohen (1954), and Polymeropoulos & Das (1975) were interested in studying the effect of droplet sizes on flame propagation in a liquid aerosol. Indeed, it is of interest to visualize eventual flame deformations by the presence of droplets on the flame front and any change to the flame propagation speed. Moreover, the laminar burning velocity of a fuel-air combination is an inherent, intrinsic parameter that may be employed in sophisticated simulations to assess the effects of an explosion under specified conditions. This parameter was evaluated via flame propagation visualization in a 1-meter-long flame propagation tube with a square cross-section of 7 cm^2. The latter was coupled with a high-speed video camera (Phantom VEO 410L) to analyze the first moments of the flame kernel growth, before touching the tube's walls. Video analyses were carried out using a model developed by Cuervo et al. (2017). The propagation speed was first estimated using models that suppose that the flame expands spherically and is driven by a one-step exothermic process with the mixture's thermodynamic parameters, such as molecular weight, specific heat, and thermal conductivity, remaining constant and allowing the estimation of the laminar burning velocity.

Values found using the flame propagation tube were then compared to calculations of the laminar burning velocity S_u^0 obtained by Silvestrini's correlation (Silvestrini et al., 2008):

$$S_u^0 = 0.11 \frac{\left(\dfrac{dP}{dt}\right)_m V^{\frac{1}{3}}}{P_m \left(\dfrac{P_m + 1}{P_0}\right)^{0.14} \left(\dfrac{P_m}{P_0}\right)^{\frac{1}{\gamma}}}$$

where dP/dt_m is the rate of pressure rise and P_m the explosion overpressure at a specific concentration, P_0 is the atmospheric pressure, and γ is the ratio of specific heats.

Such comparisons may permit to evaluate the appropriate method supplying reliable values of the laminar burning velocity of a mist cloud.

2.4 Droplet evaporation model

A droplet evaporation model, detailed in El – Zahlanieh et al. (2022), was utilized in this study in order to quantify the vapor fraction in the 20 L sphere before ignition. This model was based on the d^2-law, which is a simplified law, developed by Godsave (1953), that represents the evaporation of a single spherical droplet in a uniform-temperature environment, neglecting all exterior interactions. Some modifications were applied to the d^2-law in order to take into account a cloud of mists, its turbulence level, and the possible saturation that might occur in the confined vessel. The main equations used for this model are:

$$d^2 = d_0^2 - Kt$$

where d is the droplet diameter at time t, d_0 is the initial droplet diameter, and K is the evaporation rate constant and is calculated as follows:

$$K = 8D\frac{\rho}{\rho_l}\ln(1 + B_T)$$

where D is the vapor diffusion coefficient, ρ and ρ_l are the vapor and liquid densities respectively, and B_T is the thermal transfer Spalding number.

In order to take into account the turbulence level, K_t is calculated:

$$K_t = K\left(1 + 0.0276Re^{\frac{1}{2}}Sc^{\frac{1}{3}}\right)$$

where Re and Sc are the Reynolds and Schmidt numbers respectively.

Finally, combustion was also considered by including the combustion enthalpy, the oxygen mass fraction in the surrounding environment, and the mass stoichiometry coefficient in the calculation of the thermal and mass transfer Spalding numbers.

3. Results and discussion

3.1 Explosion severity tests

For a range of concentration reaching about 160 g.m^{-3}, diesel mists were tested and exhibited explosivity as of 92 g.m^{-3} at 27 °C. However, the same tests were performed with a new batch of diesel from the same supplier, and no explosion took place under the same conditions. This raised the question about the petroleum cut and the vapor fraction of commercial fuels. Isooctane-diesel blends were then tested and showed an increase in explosivity parameters from 4.2 bar and 31 bar.s^{-1} to 5.1 bar and 100 bar.s^{-1} as the isooctane percentage was increased from 5 to 15 %$_{v/v}$ respectively. Complementary tests will be performed on high turbulence levels and higher concentrations.

The same tests were also carried out on Jet A1 and isooctane blends. As seen in Figure 2, the addition of isooctane increased both P_m and dP/dt_m considerably. Another observed influence would be on the lower explosive limit which shifted from about 80 g.m^{-3} for Jet A1 only to about 45 g.m^{-3} for Jet A1 + 25 %$_{v/v}$ isooctane. Indeed, the presence of an increased vapor fraction surrounding the droplets facilitated the ignition of the mist cloud. As it can also be seen, the most noticeable difference is observed in the rates of pressure rise at relatively high mist concentrations, showing the influence of an important vapor fraction on the kinetics of the mist explosion.
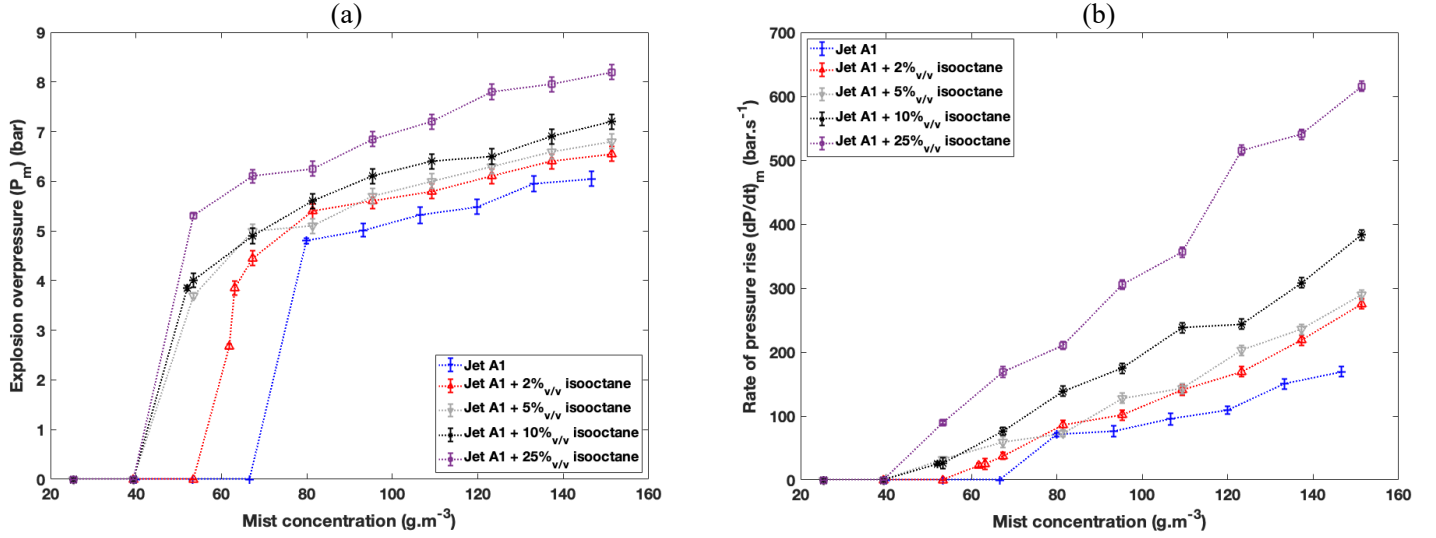
Fig. 2. *Evolution of the explosion overpressure (a) and the rate of pressure rise (b) with mist concentration and isooctane volume percentage*

3.2 Ignition time

For a total mist concentration of about 125 g.m^{-3}, the time necessary to ignite the mist cloud of the five blends was compared. An ignition delay time (IDT) is usually a crucial parameter used by engine designers and can be usually measured at high temperatures and pressures in a shock tube. This parameter is an important macro indicator of a fuel's reactivity (Khaled et al., 2017). When a certain fuel combination is subjected to specific thermodynamic circumstances of pressure and temperature, it takes a certain amount of time for it to oxidize and produce heat. In the current study, this ignition time $\tau_{ignition}$ is defined as the time needed for the mist cloud to ignite and reach a maximum rate of pressure rise P_m after the actuation of the ignition source in the 20 L sphere (see Figure 3).
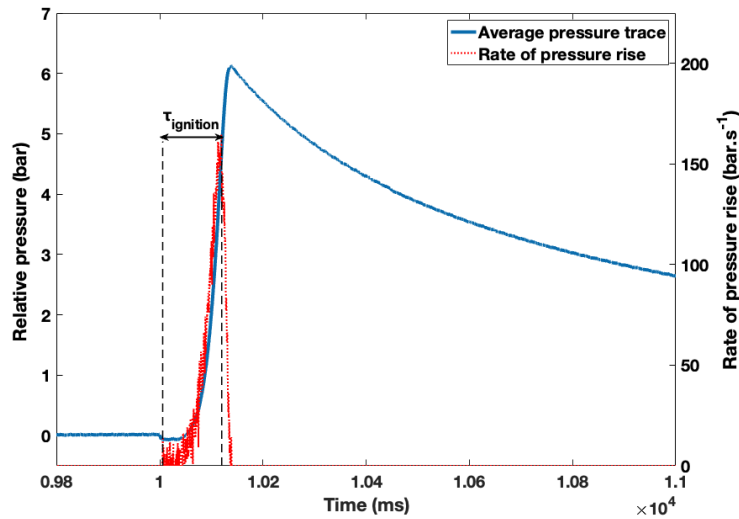

Fig. 3. *Evolution of the explosion pressure and the rate of pressure rise with time*

Figure 4 demonstrates the pressure-time evolution of Jet A1 mist alone, as well as Jet A1-isooctane blends of varying isooctane percentages (2, 5, 10, and 25 %$_{v/v}$). These tests were all performed at a sphere temperature of 27 ± 0.5 °C and with a 100 J permanent spark that lasts for about 445 ms. The decrease in $\tau_{ignition}$ was evident as the isooctane volume percentage increased, showing a significant enhancement and an acceleration of the reactivity with faster rates of pressure rise. Indeed, as shown

in Table 2, a Jet A1 mist cloud of 125 $g.m^{-3}$ required 121 ms after the actuation of the spark to ignite and reach 161 $bar.s^{-1}$. On the other hand, 25 %$_{v/v}$ of isooctane reduced this duration to about its half (59 ms) to reach a dP/dt_m about three times faster (516 $bar.s^{-1}$). Another observed influence is that on the explosion overpressure, which increases from 5.9 bar to 7.8 bar which could be explained by the higher energy density of isooctane and the domination of a high-temperature energy release governing its ignition (Dumitrescu et al., 2011).
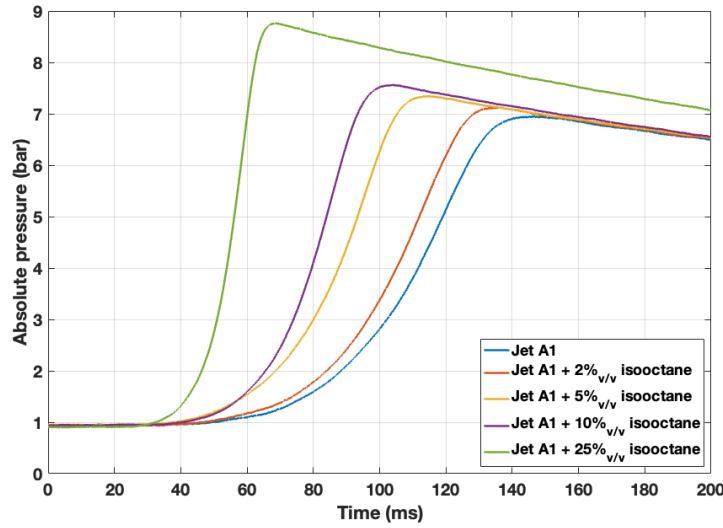

Fig. 4. *Evolution of the explosion pressure for Jet A1 and isooctane blends with time*

Table 2: *Evolution of the ignition delay time as a function of isooctane volume percentage (mist mass concentration 125 $g.m^{-3}$)*

Fuel blend	$\tau_{ignition}$ (ms)	P_m (bar)	dP/dt_m (bar.s^{-1})
Jet A1	121	5.9	161
Jet A1 + 2%$_{v/v}$ isooctane	113	6.1	170
Jet A1 + 5%$_{v/v}$ isooctane	94	6.3	203
Jet A1 + 10%$_{v/v}$ isooctane	85	6.5	244
Jet A1 + 25%$_{v/v}$ isooctane	59	7.8	516

3.3 Minimum ignition energy

Along with the ignition time, the lower explosive limit, and the thermo-kinetic explosion parameters, the minimum ignition energy was influenced by the addition of isooctane. A high-voltage spark ignition system with control of both the voltage and the spark duration was designed to measure this parameter. This system consisted of a Brandenburg 3590-1320 DC/DC converter with a 12 V to 10 kV voltage range, total power of 5 W, and a maximum input current of 0.5 mA. The output of this converter may be changed, allowing for fine-tuning of the energy sent to the mist cloud. To get an exact estimate of the provided ignition energy, the total spark duration and the continuous delivered current would be determined. Table 3 shows the evolution of the MIE with the increase of isooctane volumetric percentage in a 65 $g.m^{-3}$ Jet A1-isooctane blend. As it can be seen, increasing isooctane in the mist cloud renders it easily ignitable as the MIE decreased from a value greater than 900 mJ for Jet A1 mist to a value less than 160 mJ when the mixture contained 25 %$_{v/v}$ of isooctane. This can be explained by the help of isooctane molecules in facilitating the flame kernel's growth and propagation within the mist cloud.

Table 3: *MIE of Jet A1 – isooctane blends (mist mass concentration of 65 g.m^{-3})*

Fuel blend	MIE (mJ)
Jet A1	> 900
Jet A1 + 2%$_{v/v}$ isooctane	630
Jet A1 + 5%$_{v/v}$ isooctane	380
Jet A1 + 10%$_{v/v}$ isooctane	250
Jet A1 + 25%$_{v/v}$ isooctane	< 160

3.4   Evaporation model

Following the evaporation model based on the d^2 law and detailed in Section 2.4, Figure 5 represents the ratio of the vapor fraction and the corresponding lower explosive limit of both Jet A1 and isooctane mists. As it can be seen, at 300 K corresponding to 27 °C, the amount of Jet A1 vapor in a confined mist cloud, of a mean diameter of 8 µm, is not sufficient to sustain an explosion; nonetheless, at this concentration (3 g ➔ ~ 150 g.m^{-3}) an explosion occurs (See Figure 2) showing the contribution of the Jet A1 mist. A big difference is seen for the same mass of injected isooctane as its LEL is easily reached at this temperature.
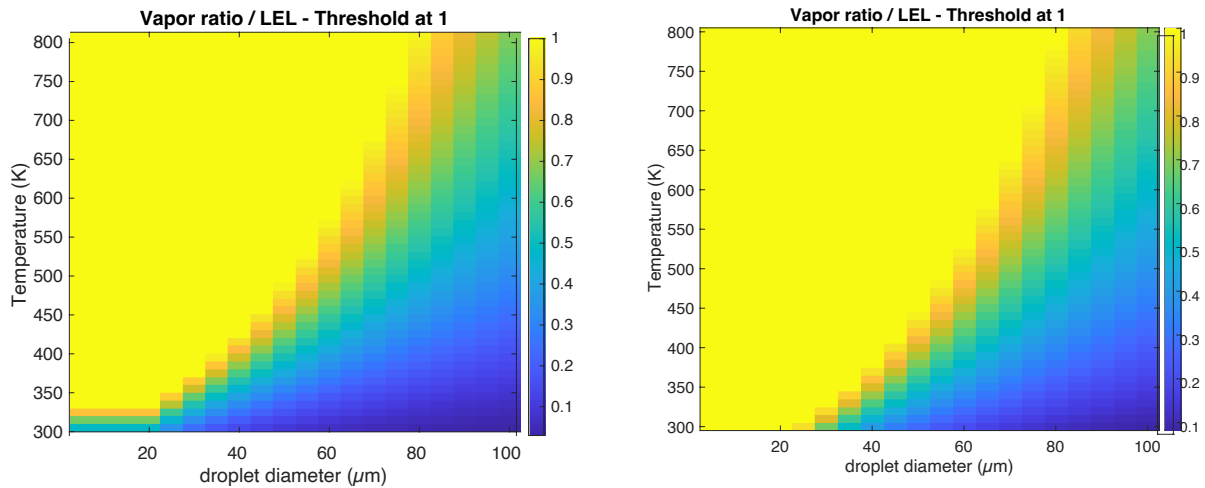

Fig. 5. *Evolution of the vapor fraction / LEL ratio as a function of ambient temperature and droplet diameter for 3 g injected of: (a) Jet A, (b) isooctane*

Current work is in progress to apply the evaporation model on a multicomponent mist cloud and link findings to experimental data.

3.5   Hybrid mixtures

Interest in hybrid dust-gas explosions has been rising throughout the years. Nevertheless, a hybrid mixture can be defined as an aerosolized liquid and gas mixture capable of being ignited and can indeed trigger an explosion. Moreover, it was seen as interesting to highlight the contribution of the mist in a mist-gas cloud to its explosivity. For these reasons, experiments were first performed at a sphere temperature of 27 ± 0.5 °C while varying Jet A1 mist concentrations between 67 and 120 g.m^{-3} to quantify the explosion severity of hybrid mixtures containing 3%$_{v/v}$ of methane. As seen in Table 4, the addition of a low percentage of methane first influenced the LEL of the mist cloud by facilitating ignition at a concentration lower than 80 g.m^{-3}. Rates of pressure rise were also seen to accelerate by at least 3.6 times their initial values, even though the percentage of CH$_4$ did not exceed its LEL which is about 5.5 %$_{v/v}$. An explosion occurring when both components were found in lower quantities than their LELs shed light on the importance of understanding the explosion behavior of gas-mist hybrid mixtures and determining the explosion driving regime. It is indeed important to

determine whether a mist is sufficient to drive an explosion even when the gas content is not enough. Methane concentrations were therefore varied between 0 and 12 $\%_{v/v}$ and Jet A1 mists between 0 and 120 g.m^{-3}. The same level of turbulence was maintained throughout the series of experiments to ensure that no influence, other than the Jet A1 – CH$_4$ mixture composition, occurred on the explosivity.

Figure 6 represents a bubble chart expressing the rates of pressure rise obtained for varying concentration to explosive limits ratios as inspired by Russo et al. (2012), who evaluated the explosion severity of methane and nicotinic acid.

Here we differentiate between the LEL of CH$_4$ expressed in volumetric percentage, experimentally measured to be 5.5 $\%_{v/v}$, and the minimum explosion concentration (MEC) of Jet A1 mist expressed in g.m^{-3}, experimentally measured to be 80 g.m^{-3}. As can be seen in Figure 6, the diameter of dP/dt$_m$ circles is proportional to their values raging between 52.5 bar.s^{-1} to 613 bar.s^{-1}. The figure also demonstrates the existence of five different explosion regimes. A "mist-driven explosion" zone can first be identified for explosions taking place at mist concentrations above the MEC and CH$_4$ concentrations below the LEL. Inversely, when the CH$_4$ concentration is maintained above its LEL, and the contrary for Jet A1, the explosion becomes more "gas-driven". On the other hand, when both concentrations are above the lower limits, both fuels are considered to have contributed to the explosion leading to a "dual-fuel explosion" zone. Note that explosions with the same CH$_4$ concentration were more severe when more Jet A1 was introduced to the mixture, demonstrating the contribution of the mist cloud. Finally, the last two zones were seen to be divided into a "no explosion" zone and a "synergic explosion" zone. The latter was identified because it was seen that the interaction of the two components resulted in a total impact bigger than the sum of their individual effects, even when below both their flammability limits. The former can be separated from the explosion regime by either Le Chatelier's mixture flammability limit rule (Mashuga & Crowl, 2000), usually applied for homogeneous gas mixtures, or the Bartknecht curve (Addai et al., 2016), usually applied for hybrid dust-gas mixtures.

Le Chatelier's law, which shows a linear relationship between the MEC of the mist and the LEL of the gas both weighed by their concentrations, is as follows:

$$LEL_{mixture} = \frac{1}{\dfrac{C_{mist}}{MEC_{mist}} + \dfrac{y_{CH_4}}{LEL_{CH_4}}}$$

Bartknecht curve, which shows that, by a second order equation, the MEC of the hybrid mixture decreases with increasing gas concentrations, is as follows:

$$MEC_{mixture} = MEC_{mist} \left(\frac{y_{CH_4}}{LEL_{CH_4}} - 1 \right)^2$$

Figure 4 shows that the Bartknecht curve may better delimit the two zones as no explosions occurred under the curve. Nevertheless, complementary tests are required to better quantify and understand liquid-gas explosions. Preliminary experiments on hybrid mixtures have, however, highlighted the role that mists can take in an explosion.

Table 4: Influence of methane gas on Jet A1 mist explosions at T = 27 °C

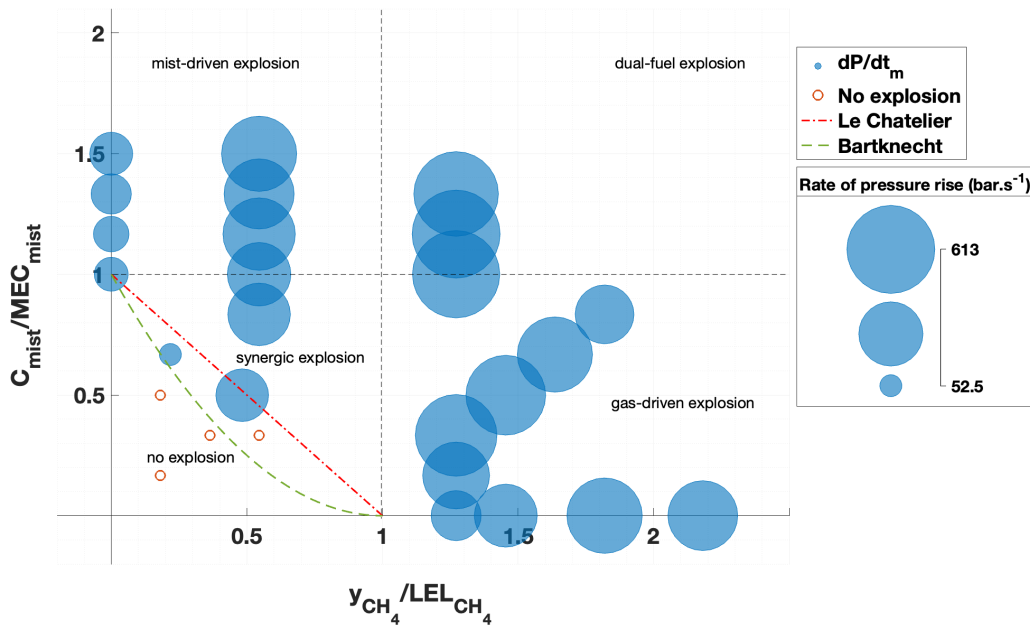|	Mist concentration (g.m^{-3})	67	80	93	107	120
P$_m$ (bar)	**Jet A1**	0	4.8	5	5.3	5.5
	Jet A1 + 3%$_{v/v}$ methane	6.5	6.7	7	7.2	7.4
dP/dt$_m$ (bar.s^{-1})	**Jet A1**	0	71	76	95	109
	Jet A1 + 3%$_{v/v}$ methane	264	274	379	350	416

Fig. 6. *Explosion experimental results as a function of Jet A1 mist and methane concentrations*

3.6   Laminar burning velocity

Calculations based on the correlation of Silvestrini allowed obtaining laminar burning velocities, as shown in Figure 7, for the Jet A1 and isooctane blends at 27 °C. Due to the dependence of S_u^0 on P_m and dP/dt_m, it follows their evolution as it increases with increasing mist concentrations and accelerates with increasing isooctane percentages. Pre-evaporated and premixed Jet A1-air mixtures were tested by Vukadinovic et al. (2013) and exhibited a laminar burning velocity of about 35 cm.s^{-1} at stoichiometric conditions and an initial temperature and pressure of 27 °C and 1 bar respectively. Such a higher value can be explained by the fact that the Jet A1 was pre-evaporated before ignition, hence facilitating the propagation of the flame.
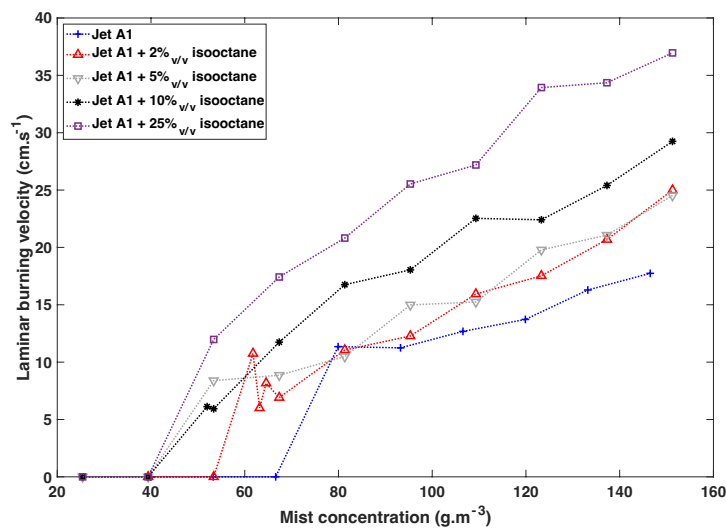

Fig. 7. *Evolution of the calculated laminar burning velocity as a function of Jet A1 - isooctane mist concentration*

Experimental values of the laminar burning velocity obtained from the flame propagation tube are currently being calculated and will be presented soon. Figure 7 demonstrates two different flame

propagations in isooctane and Jet A1 mist clouds. As it can be seen in Figure 7a, the flame front was not perfectly smoothed indicating its deformation due to present isooctane droplets. Further analyses are under development.
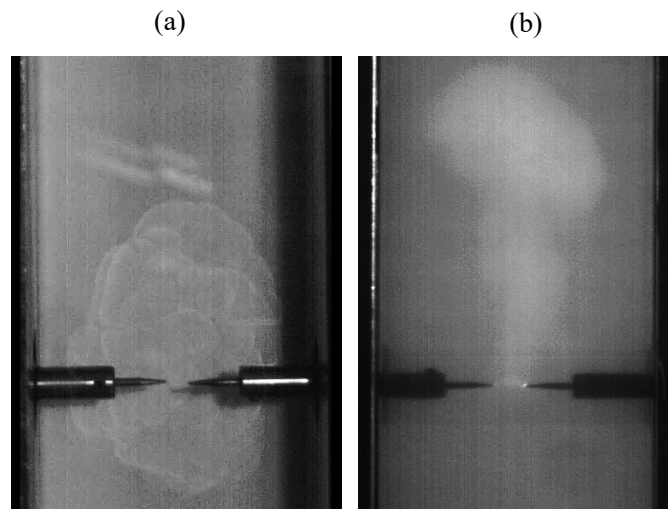

(a) (b)

Fig. 8. Flame propagation in (a) isooctane mist cloud at 120 ms ignited by a 3 J spark (b) Jet A1 mist cloud at 100 ms ignited by a 200 J spark

4. Conclusions

This study proposed a new test method that can be used for the assessment of mist ignitability and explosivity. Indeed, it was proven that, in a single apparatus, it is possible to determine the explosion overpressure P_m, the rate of pressure rise dP/dt_m, the lower explosive limit LEL, and the minimum ignition energy MIE.

Experiments showed that commercialized fuels can behave differently depending on petroleum cuts, aging, or suppliers. Tests were, therefore, conducted on B7 diesel and Jet A1 with the addition of flammable isooctane. The latter increased the explosivity of both fuels and enhanced their ignitability. Indeed, in the case of Jet A1 – isooctane blends, the LEL of the mist cloud decreased from 80 g.m^{-3} to about 45 g.m^{-3}. Another influence was the considerable acceleration of the rate of pressure rise. Moreover, a significant decrease in the MIE was observed from a value above 900 mJ for pure Jet A1 to a value below 160 mJ for Jet A1 + 25 %$_{v/v}$ isooctane. In addition, an evaporation model based on the d^2 law was developed to quantify the vapor fraction in a confined mist cloud and take into account the saturation that could take place. This model will also be applied to multicomponent droplets to be more adaptable to fuels or fuel blends. Furthermore, experiments were conducted on hybrid mixtures of Jet A1 mist and methane gas, allowing the distinction of five explosion regimes. A "no explosion" zone that is delimited by the Bartknecht curve, a synergic explosion zone where both fuels complemented each other, a mist- and a gas-driven explosion zone where the explosions were dominated by the presence of Jet A1 mists and methane gas, respectively, and finally, a dual-fuel explosion zone where both mist and gas contributed to the explosion. An interesting finding is the more severe explosions observed in the dual-fuel explosion zone, highlighting the contribution of the mist cloud. Finally, the laminar burning velocity was calculated using existing correlations and explosion severity parameters and was shown to reach values between 15 and 38 cm.s^{-1} for Jet A1 mists and Jet A1 + 25%$_{v/v}$ isooctane mist, respectively. In addition, flame propagation tests performed in a flame propagation tube will soon be used to compare to this velocity's calculated values.

Complementary analyses are under development to better quantify the contribution of the vapor fraction to the ignitability and explosivity of a fuel mist cloud.

References

Addai, E. K., Gabel, Dieter, & Krause, Ulrich. (2016). Models to estimate the lower explosion limits of dusts, gases and hybrid mixtures. *Chemical Engineering Transactions*, *48*, 313–318. https://doi.org/10.3303/CET1648053

Burgoyne, J. H., & Cohen, L. (1954). The Effect of Drop Size on Flame Propagation in Liquid Aerosols. *Proceedings of the Royal Society of London. Series A, Mathematical and Physical Sciences*, *225*(1162), 375–392. JSTOR.

Cuervo, N., Dufaud, O., & Perrin, L. (2017). Determination of the burning velocity of gas/dust hybrid mixtures. *Process Safety and Environmental Protection*, *109*, 704–715. https://doi.org/10.1016/j.psep.2017.06.009

Dumitrescu, C. E., Guo, H., Hosseini, V., Neill, W. S., Chippior, W. L., Connolly, T., Graham, L., & Li, H. (2011). The Effect of Iso-Octane Addition on Combustion and Emission Characteristics of a HCCI Engine Fueled With n-Heptane. *Journal of Engineering for Gas Turbines and Power*, *133*(11). https://doi.org/10.1115/1.4003640

Eckhoff, R. K. (2005). Chapter 3—Explosions in Clouds of Liquid Droplets in Air (Spray/Mist). In R. K. Eckhoff (Ed.), *Explosion Hazards in the Process Industries* (pp. 149–173). Gulf Publishing Company. http://www.sciencedirect.com/science/article/pii/B9780976511342500087

Eichhorn, J. (1955). Careful! Mist can explode. *Petroleum Refiner*, *34(11)*, 194–196.

El – Zahlanieh, S., Sivabalan, S., Dos Santos, I. S., Tribouilloy, B., Brunello, D., Vignes, A., & Dufaud, O. (2022). A step toward lifting the fog off mist explosions: Comparative study of three fuels. *Journal of Loss Prevention in the Process Industries*, *74*, 104656. https://doi.org/10.1016/j.jlp.2021.104656

Godsave, G. A. E. (1953). Studies of the combustion of drops in a fuel spray—The burning of single drops of fuel. *Symposium (International) on Combustion*, *4*(1), 818–830. https://doi.org/10.1016/S0082-0784(53)80107-4

Khaled, F., Badra, J., & Farooq, A. (2017). Ignition delay time correlation of fuel blends based on Livengood-Wu description. *Fuel*, *209*, 776–786. https://doi.org/10.1016/j.fuel.2017.07.095

Lees, P., Gant, S., Bettis, R., Vignes, A., Lacome, J.-M., & Dufaud, O. (2019). *Review of recent incidents involving flammable mists*. *166*, 23.

Mashuga, C. V., & Crowl, D. A. (2000). Derivation of Le Chatelier's mixing rule for flammable limits. *Process Safety Progress*, *19*(2), 112–117. https://doi.org/10.1002/prs.680190212

NTSB. (2022). *Engine Room Fire aboard Towing Vessel Miss Dorothy* (MIR-22/05; p. 15). National Transportation Safety Board. https://www.ntsb.gov/investigations/AccidentReports/Reports/MIR2205.pdf

Polymeropoulos, C. E., & Das, S. (1975). The effect of droplet size on the burning velocity of kerosene-air sprays. *Combustion and Flame*, *25*, 247–257. https://doi.org/10.1016/0010-2180(75)90091-7

Russo, P., Benedetto, A. D., & Sanchirico, R. (2012). *Theoretical evaluation of the explosion regimes of hybrid mixtures*. https://doi.org/10.3303/CET1226009

Safarov, J., Ashurova, U., Ahmadov, B., Abdullayev, E., Shahverdiyev, A., & Hassel, E. (2018). Thermophysical properties of Diesel fuel over a wide range of temperatures and pressures. *Fuel*, *216*, 870–889. https://doi.org/10.1016/j.fuel.2017.11.125

Santon, R. C. (2009). *Mist fires and explosions—An incident survey*. *155*, 5.

Shepherd, J. E., Krok, J. C., & Lee, J. J. (1997). *Jet A Explosion Experiments: Laboratory Testing*. 74.

Silvestrini, M., Genova, B., & Leon Trujillo, F. J. (2008). Correlations for flame speed and explosion overpressure of dust clouds inside industrial enclosures. *Journal of Loss Prevention in the Process Industries*, *21*(4), 374–392. https://doi.org/10.1016/j.jlp.2008.01.004

Vukadinovic, V., Habisreuther, P., & Zarzalis, N. (2013). Influence of pressure and temperature on laminar burning velocity and Markstein number of kerosene Jet A-1: Experimental and numerical study. *Fuel*, *111*, 401–410. https://doi.org/10.1016/j.fuel.2013.03.076

Willingham, C. B., Taylor, W. J., Pignocco, J. M., & Rossini, F. D. (1945). Vapor pressures and boiling points of some paraffin, alkylcyclopentane, alkylcyclohexane, and alkylbenzene hydrocarbons. *Journal of Research of the National Bureau of Standards*, *35*(3), 219. https://doi.org/10.6028/jres.035.009

Yuan, S., Ji, C., Han, H., Sun, Y., & Mashuga, C. V. (2021). A review of aerosol flammability and explosion related incidents, standards, studies, and risk analysis. *Process Safety and Environmental Protection*, *146*, 499–514. https://doi.org/10.1016/j.psep.2020.11.032